J. Biochem. 126, 738-747 (1999)

Studies on the Cell-Type Specific Expression of RBP-L, a RBP-J Family Member, by Replacement Insertion of β-Galactosidase[1]

Shigeru Minoguchi,* Toshio Ikeda,†‡ Shigeyoshi Itohara,†‡ Takeshi Kaneko,§ Hironari Okaichi,‖ and Tasuku Honjo*,[2]

**Departments of Medical Chemistry and §Morphological Brain Research, Faculty of Medicine, and †Virus Research Institute, Kyoto University, Sakyo-ku, Kyoto 606-8501; ‡Advanced Technology Development Center, RIKEN Brain Research Institute, Hirosawa 2-1, Wako, Saitama 351-0198; and ‖Department of Psychology, Doshisha University, Karasuma-Imadegawa, Kamigyo-ku, Kyoto 602-8580*

Received June 30, 1999; accepted August 2, 1999

The RBP-L gene encodes a DNA binding protein that is structurally related to RBP-J, the mammalian homolog of *Drosophila* Suppressor of Hairless. Although the RBP-L protein binds the same DNA sequence as RBP-J, the *in vivo* function of this protein remains largely unknown. In order to investigate the role of this protein, we generated RBP-L mutant mice by targeted disruption involving replacement of the protein-coding sequence in the first exon with an in-frame fusion of the *nlacZ* cDNA. The homozygous mutant mice appeared morphologically normal and fertile. Unexpectedly, we found the possible existence of additional promoter(s) downstream of the first exon whose activity was not fully disrupted in the mutant mice. The promoter upstream of the first exon is regulated in a cell type-specific manner so that transcription is active in neurons but almost inactive in lung where the downstream promoter is active. The specific expression of the β-galactosidase fusion protein was detected in layer VI of the cerebral cortex, in the pyramidal cell layer of the hippocampus, and in the granule cell layer of the dentate gyrus. Furthermore, we found that the upstream promoter activity in neurons might be regulated by some neuronal activity.

Key words: DNA binding protein, gene targeting, tissue-specific expression.

RBP-J is a unique DNA binding protein without known motifs (*1*). The structure of this protein is highly conserved during evolution from nematodes to humans (*2-6*). RBP-J binds to DNA and tethers the intracellular region of the Notch receptor, which is probably cleaved in the transmembrane region after interaction with a ligand such as Delta (*7-9*). RBP-J is ubiquitously expressed (*10*) and involved in the developmental regulation of many different cell lineages in association with Notch and Delta (*11*). The involvement of RBP-J or its orthologs in Notch signaling has been shown in nematode, fly, frog, and mammals (*3, 6, 12-16*). Thus, Notch RBP-J signaling is a developmental regulatory pathway highly conserved during evolution. RBP-J also tethers Epstein-Barr virus (EBV) nuclear antigen 2 (EBNA2), which is an essential molecule for virus-induced immortalization of human B lymphocytes (*17-20*).

We previously reported the identification of a new member of the RBP-J gene family, RBP-L, which is specifically expressed in lung, and to a much lesser extent, in spleen and brain (*21*). Since the RBP-L protein binds DNA by recognizing the same nucleotide sequence, (C/T) GTGGGAA, as RBP-J (*21, 22*), RBP-L was supposed to be involved in differentiation pathways related to Notch. However, a previous attempt to connect RBP-L with known 4 Notch proteins was unsuccessful because RBP-L does not bind to the RAM domain of Notch family proteins, which is the region involved in the interaction with RBP-J (*21, 23-25*). However, RBP-L was shown to cooperate with EBNA2 for its transactivation activity, although RBP-L shows a lower binding affinity for EBNA2 than RBP-J. Since RBP-L is specifically expressed in a limited number of organs, RBP-L is assumed to have unique and organ-specific functions in lung, brain, and spleen. Alternatively, this gene may be involved in organ-specific developmental events in these organs.

In order to assess the function of RBP-L, we employed a loss-of-function approach by inserting of the *nlacZ* reporter gene, which allows us to monitor the precise expression profile of RBP-L *in vivo*. We found a unique and complex expression profile for the RBP-L gene in lung and brain. However, insertional mutagenesis of the RBP-L gene into exon 1 failed to generate any obvious morphological or functional phenotypes. Further analysis is required to associate its interesting expression profile with the *in vivo* function of the RBP-L gene.

[1] This study was supported by grants for the COE program from the Ministry of Education, Science, Sports and Culture of Japan.

[2] To whom correspondence should be addressed. Phone: +81-75-753-4371, Fax: +81-75-753-4388, E-mail: honjo@mfour.med.kyoto-u.ac.jp

Abbreviations: DT-A, diphtheria toxin A-fragment; G418, geneticin; GST, glutathione S-transferase; Neo, neomycin resistance gene; NP40, nonidet P-40; PBS, phosphate-buffered saline; PFA, paraformaldehyde; RT-PCR, reverse transcriptase-PCR; Triton X-100, polyethylene *p-t*-octylphenyl ether; X-gal, 5-bromo-4-chloro-3-indolyl-β-D-galactopyranoside.

MATERIALS AND METHODS

Cloning and Sequencing of RBP-L Genomic DNA Clones—A cDNA fragment, encompassing the protein-coding sequence corresponding to nucleotides 1 to 1545 (*21*), was used to screen a mouse 129/Sv genomic library (Stratagene). Hybridization was performed under standard conditions (*26*). The cloned genomic DNAs were digested with appropriate restriction enzymes, subcloned into pBluescriptIIKS(−) (Stratagene), and subjected to sequencing by primer walking.

Targeting Vector Construction—The targeting vector is composed of an approximately 4-kb *Nhe*I/*Nco*I fragment of 5′-flanking and 5′-untranslated regions of the RBP-L gene, a 6.8-kb *Nhe*I fragment encompassing exons 2 to 7 of the RBP-L gene, an about 4-kb fragment of the *nlacZ* gene with an SV40 transcription termination signal and poly(A)$^+$ sequences (*27*), a 1.8-kb *pgk-neo* gene cassette (*28*), and a 1.0-kb diphtheria toxin A-fragment (DT-A) gene cassette (*28*).

Generation and Genotyping of RBP-L Mutant Mice—Cell culture and the targeting experiment were performed as described previously (*28*). E14 ES cells (5×10^7) were electroporated with a Bio-Rad Gene Pulser (800 V and 3 μF) with 30 μg of targeting vector DNA linearized with *Xho*I. Drug selection was done using 125 μg/ml G418. G418 resistant colonies were isolated and screened by digestion with *Eco*RI and hybridization with a cDNA probe (nucleotides 752 to 1014). Microinjection of ES cells into C57BL/6 blastocysts was carried out as described (*28*). Mice heterozygous for the mutation were obtained by crossing the chimeras to C57BL/6 mice. The heterozygotes were intercrossed to obtain mutation homozygotes. The genotypes of the mice were determined by Southern blot analysis.

Northern Blot Analysis—Total RNA was isolated with Trizol (Gibco). Twenty micrograms of each total RNA was electrophoresed in a 1% agarose gel and transferred to a Hybond-N+ Nylon membrane (Amersham). Hybridization was carried out under standard conditions with the cDNA probe (752 to 1014).

RT-PCR—The reverse transcriptase reaction and subsequent PCR were carried out as described previously (*21*) with the following primers. Exon 1 sense strand primers on the protein-coding or 5′-untranslated region correspond to nucleotides 1 to 20 or −76 to −57, respectively. Exon 2, 3, 3/4, 5, 6, 7, 8, and 9 sense strand primers correspond to nucleotides 44 to 63, 176 to 195, 247 to 266, 352 to 371, 477 to 496, 614 to 633, 795 to 814, and 969 to 988, respectively. Exon 6, 7, 10, 11/12, and 12 antisense strand primers correspond to nucleotides 477 to 496, 617 to 636, 1067 to 1086, 1267 to 1286, and 1543 to 1562, respectively. The β-actin primers amplify a 245-bp fragment of cDNA extending from nucleotide 183 to 427. AP14 cell RNA (*29*) was a gift from J. Takahashi and K. Tanigaki.

β-Galactosidase Staining with X-gal—Mice were anesthetized with an overdose of Nembutal, and fixed by intracardiac perfusion with a fixative solution containing 4% paraformaldehyde (PFA) in phosphate-buffered saline (PBS). The brain and lung were then postfixed by immersion in 4% PFA in PBS and washed three times with PBS. For paraffin section, samples were stained at 37°C overnight in a solution containing 1 mg/ml X-gal (5-bromo-4-chloro-3-indoyl-β-D-galactopyranoside), 5 mM potassium ferricyanide, 5 mM potassium ferrocyanide, 2 mM $MgCl_2$, 0.02% NP40, and 0.01% sodium deoxycholate, postfixed with 10% formalin in PBS, dehydrated through graded alcohols, embedded in paraffin, and sliced in 6 μm sections. Alternatively, fixed tissues were embedded in 3.5% agarose in PBS and sliced into 200 μm sections, stained at 37°C overnight in X-gal solution, and postfixed with 10% formalin in PBS.

In Situ Hybridization—*In situ* hybridization was performed as described previously (*30*). The antisense probe was transcribed from a 660-bp *Puu*II fragment (nucleotides 922–1581) of RBP-L cDNA. The hybridization signal was visualized with BM-Purple (Boehringer Mannheim).

Immunoperoxidase Staining of β-Galactosidase—Mice were anesthetized with Nembutal and perfused transcardially with 30 ml of PBS, followed by 50 ml of 3% (w/v) PFA and 0.1% (v/v) glutaraldehyde in 75%-saturated picric acid and 0.1 M sodium phosphate, pH 7.0 (PP). After the fixation, the mouse brain blocks were cryoprotected with 30% sucrose in PBS, and cut into 25-μm-thick frontal sections on a freezing microtome. For immunocytochemistry of glutaminase, mice were perfused with 50 ml of PP containing 0.2% PFA. The brain blocks were further fixed overnight at 4°C in PP containing 2% PFA (*31*).

The sections were incubated overnight with rabbit anti-β-galactosidase serum (Chemicon), diluted 1/10,000, for 1 h with 10 μg/ml of biotinylated anti-[rabbit IgG] donkey antibody (Jackson), and for 1 h with avidin-biotinylated peroxidase complex (ABC-Elite; Vector). The bound peroxidase was developed by reaction for 10–30 min with 0.02% (w/v) diaminobenzidine-4HCl and 0.001% H_2O_2 in 50 mM Tris-HCl (pH 7.6). Some sections were counterstained with 1% (w/v) Cresyl violet. In control tests made by replacing the primary antibody with normal rabbit IgG, no immunoreactivity was detected.

Double Immunofluorescence Study—The mouse sections were incubated overnight with a mixture of rabbit anti-β-galactosidase (1/2,000) and anti-GABA guinea pig serum (1/2,000; Chemicon) or anti-glutaminase mouse monoclonal IgM (MAb-120; 50 μg/ml) (*32, 33*). After rinsing with PBS containing 0.3% Triton X-100, the sections were incubated with 10 μg/ml of biotinylated anti-[rabbit IgG] donkey antibody (Chemicon). Finally the sections were incubated with a mixture of Texas Red-conjugated avidin D (5 μg/ml; Vector) and fluorescein-conjugated anti-[guinea pig IgG] donkey antibody or anti-[mouse IgM] donkey antibody (10 μg/ml; Jackson).

Immunofluorescence was observed under an epifluorescence microscope, Axiophot (Zeiss), with appropriate filter sets for fluorescein (excitation, 450–490 nm; emission 514–565 nm) or Texas Red (excitation, 530–585 nm; emission ≧615 nm). In control studies in which one of the primary antibodies was omitted or replaced with normal IgG or serum, no immunofluorescence was detected for the antibody.

Behavioral Analysis—The hidden-platform version of the Morris water maze test was performed (*34*). A circular, plastic walled pool (60 cm diameter, 31 cm height) was filled with 28 liters of water (8.5 cm height, at 23°C) made opaque white by adding milk at 3.5% (v/v). The mice could use the geometric information of objects around the pool as

distal visual cues. The water surface was lighted at 80 lux. A circular platform (5.5 cm diameter, 8 cm height) was hidden in one of the quadrants. The tracked positions of the mice were monitored with a videocamera and stored on videotape.

Mice were trained to find the hidden platform in 4 trials at 2-4 min intervals every day. In each of the 4 trials, the mice were placed in the water in a different area of the quadrants. If a mouse failed to find the platform in 1 min, the test was stopped and the mouse was placed on the platform for 15 s. After conducting the hidden-platform task for 6 days, a transfer test was performed on day 7. After removal of the platform, the mice were trained to search for the absent platform for 1 min. The dwell time in each quadrant was measured to confirm the formation of spatial memory.

RESULTS

Genomic Organization of RBP-L—To construct a targeting vector for the RBP-L gene, we screened a mouse 129/Sv genomic DNA library with an RBP-L cDNA probe and isolated several genomic DNA clones covering the complete RBP-L cDNA sequence (*21*). To analyze the genomic organization of the RBP-L gene, we determined an ~15 kb DNA sequence containing all exons and introns together with the 5′- (~2 kb) and 3′- (~1 kb) flanking regions. Comparison of the genomic and cDNA sequences revealed that the protein coding sequence is separated by 11 introns into 12 exons (Fig. 1A). The genomic sequences corresponding to the 5′- and 3′-untranslated regions of the RBP-L cDNA are not divided by any gaps. Although it is still possible that additional exons consisting of unidentified 5′- and 3′-untranslated region sequences could exist, we designate the exon containing the 5′-end of the known cDNA as exon 1. The two DNA binding domains, named regions N and C, are on exon 7 (cDNA nucleotides 614-752) and exon 9 (cDNA nucleotides 862-1014), respectively. At least four polymorphic nucleotide substitutions were found between the C57BL/6 cDNA and 129/Sv genomic sequences; a silent substitution of G (C57BL/6) to A (129/Sv) at nucleotide 471 of cDNA, two substitutions (C to T and A to G at nucleotides 1748 and 1990, respectively) in the 3′-noncoding region, and a replacement substitution of A to T at nucleotide 1102 of cDNA, which replaces the threonine at residue 367 (C57BL/6) with serine (129/Sv). The positions of eight splice sites out of eleven are completely conserved between RBP-L and RBP-J (*2, 35*). All

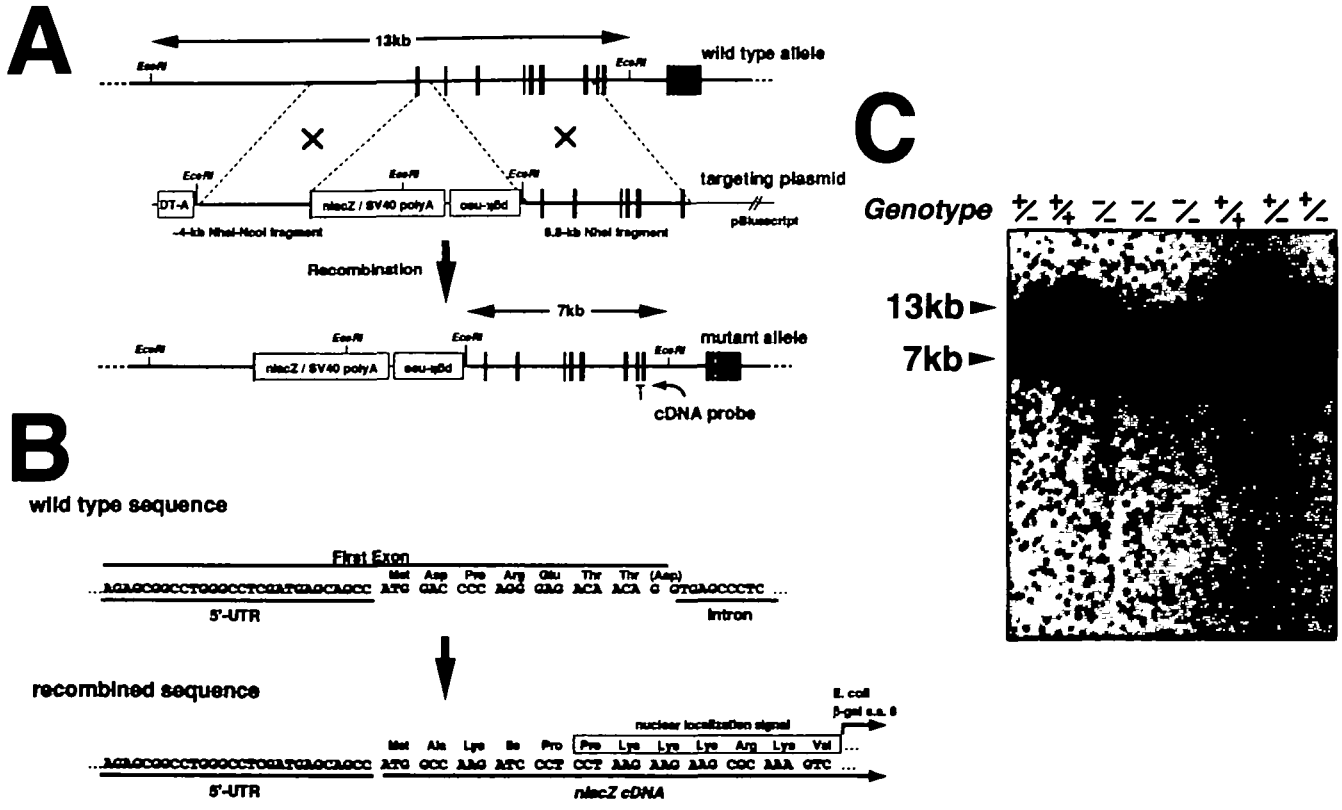

Fig. 1. **Targeted mutation at the RBP-L locus.** (A) Genomic organization and strategy for the targeted disruption of the RBP-L gene. The twelve exons are indicated as black boxes. *nlacZ*/SV40 polyA represents *nlacZ* cDNA with SV40 transcriptional termination and poly(A)$^+$ sequence. *pgk-neo* represents a neomicine resistance gene cassette. The diphtheria toxin A-fragment (DT-A) gene is used for counterselection of non-targeted events. The cDNA probe external to the vector region is shown at the bottom. (B) Sequence structure of an in-frame fusion of the *nlacZ* gene near the translational initiation site on exon 1. The protein-coding sequence on exon 1, corresponding to amino acids 2 to 8, was replaced with the *nlacZ* gene in an in-frame manner. The 5′-untranslated region (5′-UTR) of the fusion gene is derived from that of the RBP-L gene. The *nlacZ* cDNA consists of N-terminally deleted *Escherichia coli lacZ* gene with the nuclear localization signal sequence of the SV40 T antigen. (C) Southern blot analysis of offspring from the intercross of mice heterozygous for the RBP-L mutation. The 13- and 7-kb *Eco*RI fragments corresponding to the wild type and the targeted allele, respectively, were detected with the cDNA probe shown in A. +/+, +/−, and −/− represent wild type, heterozygote and homozygote for the RBP-L gene, respectively.

exon-intron boundaries are flanked by the splice consensus sequence. Although the various previously isolated cDNA clones possess poly(A)$^+$ tails without apparent polyadenylation signal-like sequences (*21*), two polyadenylation consensus sequences (AATAAA) are found at about 1.3 and 1.6 kb downstream from the termination codon in the genomic sequence.

Targeted Disruption of the RBP-L Gene—To create a null mutation in the RBP-L gene, we constructed a targeting vector in which the first 19 bp of the protein-coding sequence in exon 1 (corresponding to amino acids 2 to 8) and the 5′-half (494 bp) of the first intron are replaced with the *nlacZ* gene (a nuclear localization signal peptide-containing the *lacZ* gene with an SV40 transcription termination site and poly(A)$^+$ sequences) in an in-frame manner and the neomycine (neo)-resistant gene expression cassette in the reverse orientation (Fig. 1, A and B). A diphtheria toxin A (DT-A) gene was placed at the 5′-end of a ~4 kb genomic DNA fragment for negative selection. ES cells derived from 129/Ola mice were transfected with the linearized targeting vector by electroporation and selected in the presence of G418. To screen the isolated ES clones, we performed Southern blot analysis with a cDNA probe encompassing exons 8 and 9 (Fig. 1A). When the expected homologous recombination occurs, two novel *Eco*RI sites should be introduced into the RBP-L locus (Fig. 1A). As a result, after digestion with *Eco*RI, the cDNA probe should detect a 7-kb mutant band in addition to the 13-kb wild-type band (Fig. 1C). Southern blot analysis with the cDNA probe showed that 41 ES clones were targeted out of 351 clones isolated. Furthermore, other probes, including a neo probe, were employed to confirm correct targeting, and four ES clones containing a single targeting event were injected into blastocysts derived from C57BL/6 mice to produce chimeras. Four chimeras from one of the ES clones transmitted the RBP-L mutation through the germ line. Mice heterozygous for the RBP-L mutation showed no abnormalities and were fertile. Intercrosses of the RBP-L heterozygotes produced offspring homozygous for the RBP-L mutant allele (Fig. 1C) and the mutation was transmitted with Mendelian frequency; of 168 offsprings analyzed, 22% were wild type, 54% were heterozygous, and 24% were homozygous for the mutation. Mice homozygous mice for this mutation were viable and fertile, and showed no obvious abnormality.

Analyses of the RBP-L Transcript—In order to confirm the disappearance of RBP-L mRNA in homozygous mutant mice, we performed Northern blot analysis of total RNA from the lungs of adult mice using a cDNA probe encompassing exons 8 and 9 (Fig. 1A) because RBP-L expression is detected most abundantly in lung (*21*). The homozygous mutant mice showed an almost complete loss of RBP-L transcript expression (Fig. 2A). There was no significant reduction in RBP-L mRNA expression in RBP-L heterozygous offspring as compared with wild-type animals, suggesting that the wild-type gene may be up-regulated in heterozygous RBP-L mutants to compensate for the loss of the other allele.

Since our design of the mutant allele predicts the expression of a fused transcript containing the 5′ untranslated region of exon 1, we attempted to confirm the expression of a fusion mRNA by RT-PCR analysis employing adult lung RNA from mutant mice as a template. Unexpectedly, we

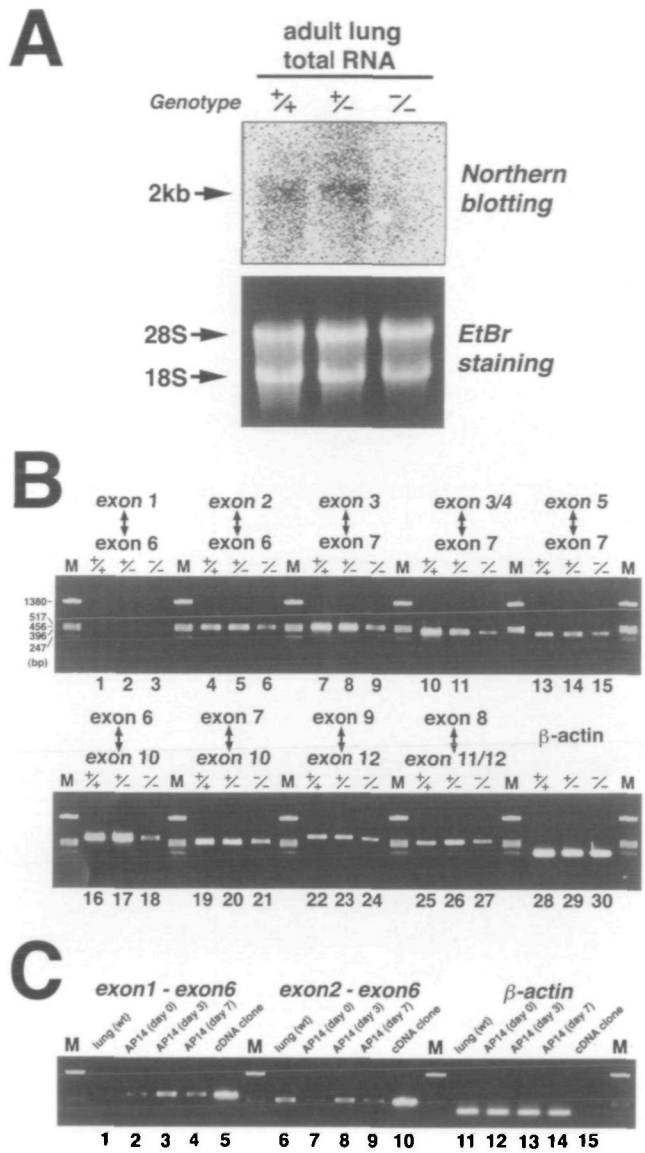

Fig. 2. **Analysis of the RBP-L gene transcript.** (A) Northern blot analysis of RBP-L mRNA in adult mouse lung. Total RNAs from wild type (+/+), heterozygous (+/−), and homozygous (−/−) mice were subjected to Northern blotting and hybridized with an RBP-L cDNA probe (upper panel). Abundant 2-kb transcripts are indicated by the arrow. Equivalent amounts of RNAs were loaded and confirmed by ethidium bromide staining before blotting (lower panel). Ribosomal RNAs are indicated by arrows. (B) RT-PCR analysis of RBP-L expression in lung. Total lung RNAs from wild type (+/+), heterozygous (+/−), and homozygous (−/−) mice were subjected to RT-PCR. RBP-L cDNA primer sets on the represented exons were used for PCR. Primer sequences are shown in "MATERIALS AND METHODS." Lanes M represent nucleotide size markers. (C) RT-PCR analysis of exon 1 expression in lung. Total RNAs from the lungs of wild type mice (lanes 1, 6, and 11), undifferentiated AP14 cells (lanes 2, 7, and 12), and differentiated AP14 cells 3 days (lanes 3, 8, and 13) or 7 days (lanes 4, 9, and 14) after differentiation initiation, were subjected to cDNA synthesis and then to PCR with the indicated RBP-L cDNA primer sets (lanes 1 to 10) or control β-actin primers (lanes 11 to 15). The exon 1 primer sequence is derived from nucleotides −76 to −57 in the 5′-untranslated region. Cloned RBP-L cDNA was used as a positive control template for PCR (lanes 5, 10, and 15).

found that RBP-L cDNA sequences encoded by exons 2 to 12 were amplified from the RNA of homozygous mutant mice, albeit to a lesser extent than in wild-type or heterozygous mice (Fig. 2B). As expected for PCR with an exon 1 primer whose sequence was derived from the protein-coding sequence of exon 1 and deleted in the mutant allele, there was no amplification in the mutant homozygotes (Fig. 2B). A greater surprise was the failure to detect PCR products amplified with the exon 1 primer even from the RNA of wild-type mouse lung. To confirm this result, we carried out extensive RT-PCR using two kinds of exon 1 primers, the one described above and another from the 5′-untranslated region (nucleotides −76 to −57), paired with various antisense primers in the downstream exons. The resulting amplification showed only trace or undetectable amounts of PCR products (data not shown).

To confirm that exon 1 can be transcribed, we attempted to detect exon 1-containing PCR products employing RNA from other sources and found that exon 1 is significantly transcribed in neuronal stem cells, AP14, derived from adult rat hippocampus (Fig. 2C). AP14 is a spontaneously immortalized, multipotent cell line that can differentiate into neurons, astrocytes, and oligodendrocytes *in vitro* (*29*). Although RT-PCR with RNA from undifferentiated AP14 cells detected small but significant amounts of RBP-L mRNA, the mRNA expression was markedly augmented 3 days after the differentiation was inducted. Seven days after induction, the augmentation was reduced (Fig. 2C). Since RBP-L mRNA expression in adult brain was restricted to neurons and not present in glial cells, as shown

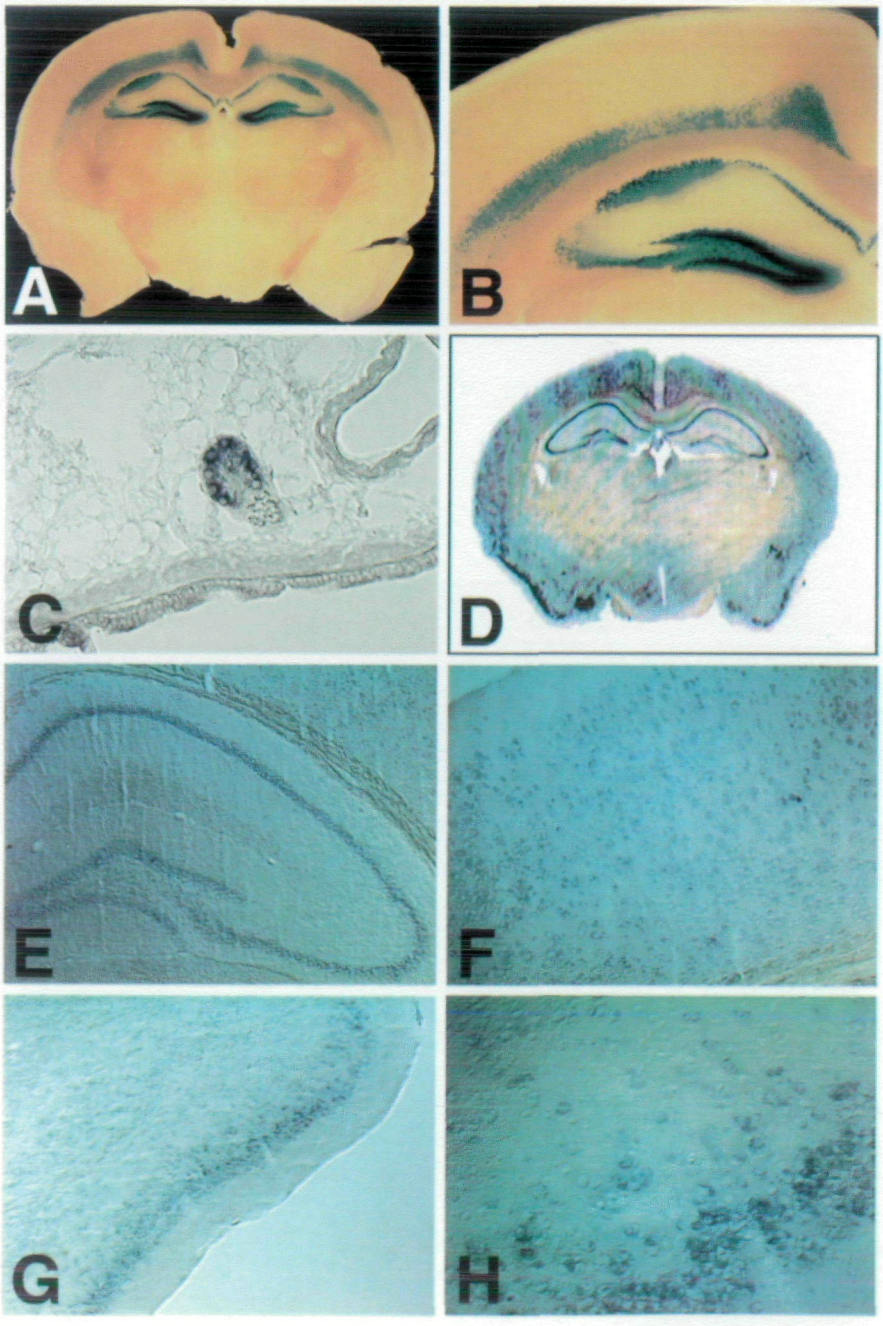

Fig. 3. **Histological analyses of RBP-L expression.** (A and B) β-Galactosidase staining of adult brain from homozygous mutants with X-gal. β-Galactosidase expression is localized at the pyramidal cell layer in the hippocampus, the granule cell layer in the dentate gyrus, and layer VI around the neo- and mesocortical regions in the cerebral cortex. (C) *In situ* hybridization analysis of RBP-L expression in the lungs of wild type adult mice. An RBP-L signal was detected in the trachyal gland. (D-H) *In situ* hybridization analysis of RBP-L expression in the brains of wild type adult mice. RBP-L mRNA was detected in the pyramidal cell layer of the hippocampus and the granule cell layer of the dentate gyrus (D and E). In the cerebral cortex, hybridization signals were evenly distributed among the six layers (D and F). Strong signals around layer II were also detected in the piriform cortex (D, G, and H).

below, the combined results imply a transient induction of RBP-L expression during differentiation to neuronal lineages. It is important to note that the time course and levels of PCR amplified products from AP14 RNA using the exon 1 sense primer with the exon 6 antisense primer were similar to those using the exon 2 sense primer with the common exon 6 primer (Fig. 2C). In contrast, a transcript containing the exon 1 sequence was not detectable in adult lung RNA under the same PCR conditions. Exon 2 was again confirmed to be transcribed in lung (Fig. 2C). These results show that exon 1 is likely to be transcribed in a neuronal cell-specific manner.

Since the mutant allele carries a transcription termination signal (SV40 polyA in Fig. 1A, Ref. *27*) between of exon 1 and 2, it is likely that there is an additional promoter downstream of exon 1. This downstream promoter is likely to be active in lung whereas the upstream promoter appears to be inactive or weakly active in lung but active in neurons. In the mutant lung, the expression of the exon 2 transcript without exon 1 was significantly reduced to a level undetectable by Northern blot hybridization, which could be explained if the deletion of the 5′-half of the first intron partially disturbs the putative downstream promoter activity.

Expression of nlacZ in Mutant Mice—To analyze *nlacZ* gene expression, we performed β-galactosidase staining of lung and brain from adult mutant heterozygotes and homozygotes. We looked extensively but failed to detect β-galactosidase-positive cells in lung (data not shown), consistent with the fact that exon 1-containing transcripts are absent from lung, probably because the upstream promoter is almost inactive in lung (Fig. 2). On the other hand, specific staining patterns were observed in the brains of heterozygous and homozygous mutant mice. The staining

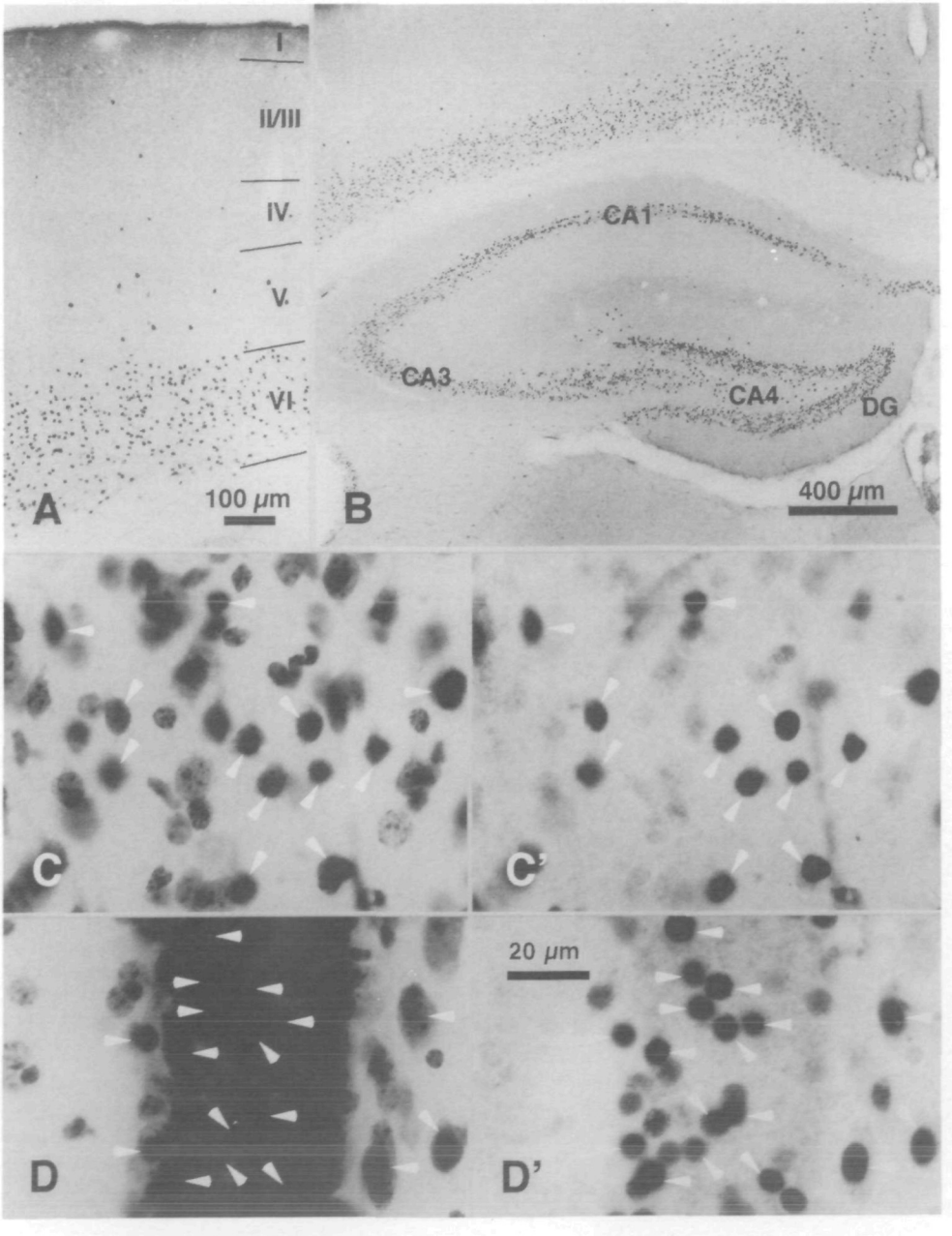

Fig. 4. **RBP-L-expressing neurons in the cerebral cortex and hippocampal formation.** Many β-galactosidase-immunoreactive neurons were found in layer VI of the neocortical regions (A, C, and C′), in the pyramidal cell layer of the hippocampus (B), and in the granule cell layer of the dentate gyrus (B, D, and D′) of knock-out-mice. C and D: The sections were counterstained for Nissl after immunoperoxidase staining with diaminobenzidine, and photographed under conventional green light. C′ and D′: the same regions were photographed under light passed through a filter with a band path around 450 nm to suppress the color of counterstaining. Arrowheads indicate β-galactosidase-immunoreactive neurons (C, C′, D, and D′). Note that β-galactosidase is designed to localize in cell nuclei.

patterns in homozygotes, as shown in Fig. 3, A and B, were indistinguishable from those in heterozygotes. β-Galactosidase-positive cells in brain were mostly confined to the pyramidal cell layer in the hippocampus, the granule cell layer in the dentate gyrus, and layer VI around the cortical sensory center in the cerebral neocortex.

Analysis of RBP-L Gene Expression in Wild-Type Mice—To investigate whether *nlacZ* expression patterns in mutant mice are in agreement with authentic RBP-L expression patterns in wild-type mice, we performed *in situ* hybridization analysis for RBP-L mRNA expression in lung and brain of wild-type adults. We used a cRNA probe encompassing exons 9 to 12, which should detect transcripts with or without exon 1. In lung, strong RBP-L mRNA expression was seen localized at the trachyal glands (Fig. 3C). This result is in agreement with the above conclusion that the upstream promoter driving *nlacZ* mRNA expression in the lung is almost inactive, but that the downstream mRNA starting from exon 2 is actively expressed by the putative downstream promoter. In brain, RBP-L mRNA was detected in areas broader than those of *nlacZ* expression. RBP-L mRNA expression in the pyramidal cell layer of the hippocampus and the granule cell layer of the dentate gyrus is in good agreement with the *nlacZ* expression pattern (Fig. 3, A and D). Although β-galactosidase-positive cells in the cornu ammonis were relatively abundant in the CA1 region (Fig. 3B), RBP-L mRNA expression was seen uniformly in the pyramidal regions (Fig. 3E). In the cerebral cortex, hybridization signals were evenly distributed among the six layers in contrast to *nlacZ* expression, which was confined to layer VI (Fig. 3, B and F). Strong hybridization signals in layer II were also apparent in the piriform cortex (Fig. 3, G and H). These results taken together suggest that in brain both the upstream and downstream promoters of RBP-L are active, but that they have different regional activities.

Immunocytochemistry for β-Galactosidase—In order to determine the type of cells that express RBP-L in brain, we examined the brain tissues of RBP-L knock-out mice immunocytochemically using specific antibodies against β-galactosidase. β-Galactosidase immunoreactivity was seen exclusively in the cell nuclei of the cerebral cortex and hippocampus (Fig. 4). Immunoreactive nuclei were apparently large and surrounded by Nissl bodies (Fig. 4, C, C′, D, and D′), indicating them to be neuronal. In the cerebral neocortex, β-galactosidase-immunoreactive neurons were distributed densely in layer VI and sparsely in layers II to V (Fig. 4A) of the frontoparietal and occipital neocortical regions and cingulate mesocortical regions. In contrast, the β-galactosidase immunoreactivity was weak in the perirhinal, piriform, and entorhinal regions. In the hippocampal formation, β-galactosidase-immunoreactive neurons were distributed mainly in the pyramidal cell layer of the cornu ammonis and the granule cell layer of the dentate gyrus (Fig. 4B). It was unexpected that only a subset of granule cells express β-galactosidase immunoreactivity (Fig. 4, D and D′) because granule cells in the dentate gyrus are thought to comprise a homogeneous population of neurons. The heterogeneous expression in this homogeneous neuronal cluster suggests that RBP-L is not a constitutional gene determining the general characteristics of granule cells, but an activity-dependent gene.

We further attempted to reveal the chemical characteristics of RBP-L expressing neurons in knockout mice using a

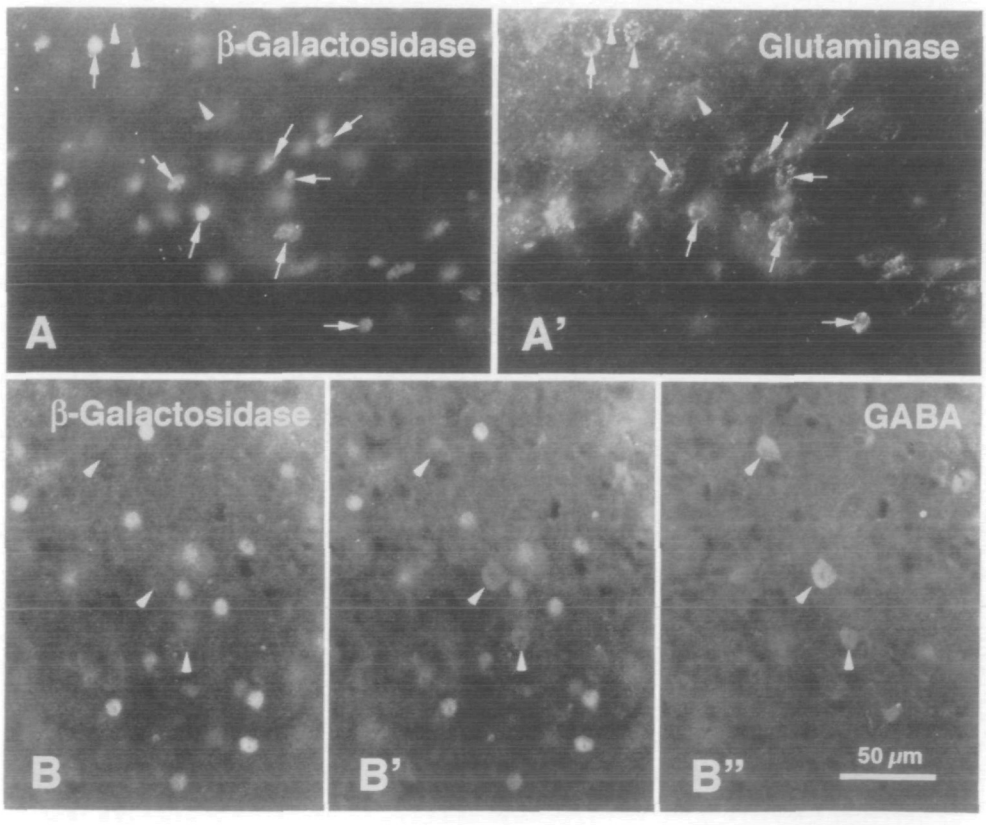

Fig. 5. **Glutaminase and GABA immunofluorescence in RBP-L-expressing neocortical neurons.** A and A′, or B-B″ were taken from a single site with the epifluorescence microscope under different excitation wavelengths; Texas Red for β-galactosidase immunoreactivity (A and B), and fluorescein for glutaminase (A′) or GABA immunoreactivity (B″). Photograph B′ was taken by double exposure for Texas Red and fluorescein. Arrows indicate glutaminase-immunopositive neurons expressing β-galactosidase immunoreactivity (A and A′). Arrowheads point to glutaminase-immunoreactive (A and A′) or GABA-immunoreactive (B-B″) neurons showing no immunoreactivity for β-galactosidase. Bar = 50 μm.

double immunofluorescence method (Fig. 5). In layer VI of the neocortical regions, many β-galactosidase-immunoreactive neurons showed glutaminase immunoreactivity (Fig. 5, A and A′), a marker for glutamatergic pyramidal neurons in the cerebral cortex (*36, 37*). In contrast, no β-galactosidase-immunoreactive neurons were positive for GABA (Fig. 5, B, B′, and B″). Similar results were obtained in the hippocampal regions. From these results we conclude that the RBP-L exon 1-β-galactosidase fusion protein is expressed exclusively in glutamatergic excitatory neurons.

Furthermore, there are glutaminase-positive, β-galactosidase-negative neurons (arrowheads in Fig. 5, A and A′), suggesting that only a subset of the layer VI pyramidal neurons express RBP-L. This is in good agreement with the heterogeneous expression in granule cells of the dentate gyrus (Fig. 4, D and D′). Taken together, the upstream promoter activity of the RBP-L gene in neurons could be associated with some neuronal activities.

DISCUSSION

In this study, we used a loss-of-function approach to evaluate the role of the transcription factor RBP-L in mouse. We generated a mutant allele with a 513-bp deletion, in which the in-frame fusion of *nlacZ* and the neo cassette are inserted. Mice homozygous for this mutation displayed morphologically and histologically normal phenotypes. A possible explanation for the absence of obvious phenotypes is that the mutation is not a null mutation. In fact, leaky expression of exons 2 to 12 from the mutant allele was observed even in the mutant homozygotes, suggesting the possible existence of an additional promoter between exons 1 and 2 whose activity was not fully disrupted in the mutant allele. These transcribed exons could form functional transcripts encoding truncated forms or splicing variants of RBP-L. For example, the putative mRNA comprising of exons 2 to 12 theoretically encodes an N-terminally truncated form using the methionine residue in exon 4 as a cryptic translation starting site. This truncated form maintains DNA binding domains and could compensate for the absence of the full-length protein in mutant mice. In practice, transcripts containing exons 2 to 12 but not exon 1 are expressed in the lungs of wild type mice, suggesting that the 5′-truncated transcript may play some specific roles *in vivo*. Although we cannot completely exclude the possibility that the expression of exons 2-12 is due to differential splicing, this is unlikely because the fused *nlacZ* cassette is followed by a strong transcription terminator (SV40 polyA). There is another possibility that different transcription starting sites driven by the common upstream promoter are employed in a cell type-specific manner. However, the deletion and the large insertion sequence in the mutant allele may make it difficult for the upstream promoter to maintain proper regulation of transcriptional initiation far downstream from the promoter in the mutant allele.

The *nlacZ* expression from the upstream promoter in lung and brain shows patterns that overlap partially with the expression of RBP-L mRNA exons 9 to 12 detected by *in situ* hybridization, suggesting that the two promoters are used differentially (Fig. 3). In addition, the upstream promoter activity in glutamatergenic excitory neurons appears to be regulated by some neuronal activities (Figs. 4 and 5). The first exon is transcribed in a neural precursor cell line, the pyramidal cell layer in the hippocampus, the granule cell layer in the dentate gyrus, and layer VI in the cerebral neocortex, but not in lung, indicating the regulated usage of exon 1 in a cell type- or tissue-specific manner.

The unique expression profiles of RBP-L transcripts in brain suggest their role in some brain functions. Especially, the rather specific expression of exon 1-containing transcripts encoding the β-galactosidase fusion protein in glutamatergic pyramidal neurons in layer VI of the cerebral cortex, hippocampus, and dentate gyrus is worth noting (Fig. 4). Furthermore, only a subset of glutamatergic neurons express RBP-L exon 1 transcripts, suggesting its regulation is associated with neuronal activities (Figs. 4 and 5). We therefore performed the Morris maze test to look for possible defects in the brain functions of mutant mice. Eight homozygotes were examined for spatial relations learning among distal visual cues around the pool to find a hidden platform. A decrease in the escape latency to the platform represents the formation of spatial memory. Mutant mice showed a progressive decrease in latency comparable to 8 control siblings (data not shown). After the hidden-platform test, the trained mice were subjected to a transfer test in which they tried to find the removed platform by swimming using spatial memory formed in the previous task. If mice have developed a navigational strategy, they should spend a longer time at the target place where the platform had existed. Therefore, we measured the dwell time in each quadrant of the pool. In this test, the mutants spent greater amounts of time in the target quadrant, as did the controls. The dwell times in each quadrant were similar for both mutant and control mice (data not shown). In conclusion, the mutant mice did not show significantly impaired behavior in learning these tasks. However, it is still possible that the mutant allele contributes to some defects in higher orders of brain function that we cannot measure adequately. It is important to construct and analyze other RBP-L mutant alleles, including the null mutation, to reveal other requirements for this gene. In addition, we need more sophisticated quantitative tests for higher order brain functions.

In our previous report, the RBP-L protein did not show any significant interaction with the RAM domains of the four Notch family members (*21, 24*). As described above, targeted disruption of the RBP-L gene produced no apparent developmental defects, but the present mutant still expresses an alternate form of RBP-L transcript. To further investigate whether RBP-L is involved in Notch signaling or not, we examined the protein-protein interactions of RBP-L and RBP-J with the cdc10/ankyrin repeats of four Notch family members because RBP-J is known to bind Notch through the cdc10/ankyrin repeats as well as through the RAM domain (*12, 14, 38*). The six-cdc10/ankyrin repeat fragments of Notch1, 2, 3, and 4 were fused to a GST protein (GST-ANK). Bacterially expressed GST-ANK fusion proteins were immobilized on glutathione-agarose beads and used to pull-down ^{35}S-labeled *in vitro* translated RBP-L or RBP-J. We found that RBP-J interacts with all of the GST-ANK fusions, whereas none of the GST-ANK fusions showed significant interaction with the RBP-L protein (data not shown). The combined results of the developmental normality of the mutant mice with the absence of an interaction with the cdc10/ankyrin repeats,

suggests that RBP-L is not a downstream signaling molecule of Notch.

Analysis of the F2 backcross offspring generated from C57BL/6 backcrosses of F1 heterozygous offspring between 129/Ola-derived heterozygous ES cells and wild type C57BL/6 mice, revealed a close linkage between the RBP-L mutant allele and the agouti coat-color phenotype. Of 89 F2 backcross offspring heterozygous for the RBP-L mutation, 86 showed agouti coat-color and only 3 were non-agouti plain black. Of 90 F2 backcross wild type mice, 85 were non-agouti and only 5 were agouti. In total, eight recombination events took place between the RBP-L and agouti gene loci during 179 meioses. Fluorescent *in situ* hybridization mapping has located the human homolog of RBP-L to human chromosome 20q13.1 (*39*), which is known to be in a large region syntenic with distal mouse chromosome 2, where the agouti gene is also known to be located. These results suggest that the RBP-L gene is located at a 4.5 cM interval from the agouti gene locus on mouse chromosome 2.

REFERENCES

1. Honjo, T. (1996) The shortest path from the surface to the nucleus: RBP-Jκ/Su(H) transcription factor. *Genes Cells* **1**, 1-9
2. Amakawa, R., Wu, J., Ozawa, K., Matsunami, N., Hamaguchi, Y., Matsuda, F., Kawaichi, M., and Honjo, T. (1993) Human Jκ Recombination signal binding protein gene (IGKJRB): Comparison with its mouse homologue. *Genomics* **17**, 306-315
3. Christensen, S., Kodoyianni, V., Bosenberg, M., Friedman, L., and Kimble, J. (1996) *lag-1*, a gene required for *lin-12* and *glp-1* signaling in *Caenorhabditis elegans*, is homologous to human CBF1 and *Drosophila* Su(H). *Development* **122**, 1373-1383
4. Furukawa, T., Kawaichi, M., Matsunami, N., Ryo, H., Nishida, Y., and Honjo, T. (1991) The *Drosophila* RBP-Jκ gene encodes the binding protein for the immunoglobbulin Jκ recombination signal sequence. *J. Biol. Chem.* **266**, 23334-23340
5. Matsunami, N., Hamaguchi, Y., Yamamoto, Y., Kuze, K., Kangawa, K., Matsuo, H., Kawaichi, M., and Honjo, T. (1989) A protein binding to the Jκ recombination sequence of immunoglobulin genes contains a sequence related to the integrase motif. *Nature* **342**, 934-937
6. Wettstein, D.A., Turner, D.L., and Kintner, C. (1997) The *Xenopus* homolog of *Drosophila* Suppressor of Hairless mediates Notch signaling during primary neurogenesis. *Development* **124**, 693-702
7. Jarriault, S., Brou, C., Logeat, F., Schroeter, E.H., Kopan, R., and Israel, A. (1995) Signalling downstream of activated mammalian Notch. *Nature* **377**, 355-358
8. Kopan, R., Schroeter, E.H., Weintraub, H., and Nye, J.S. (1996) Signal transduction by activated mNotch: importance of proteolytic processing and its regulation by the extracellular domain. *Proc. Natl. Acad. Sci. USA* **93**, 1683-1688
9. Schroeter, E.H., Kisslinger, J.A., and Kopan, R. (1998) Notch-1 signalling requires ligand-induced proteolytic release of intracellular domain. *Nature* **393**, 382-386
10. Hamaguchi, Y., Yamamoto, Y., Iwanari, H., Maruyama, S., Furukawa, T., Matsunami, N., and Honjo, T. (1992) Biochemical and immunological characterization of the DNA binding protein (RBP-Jκ) to mouse Jκ recombination signal sequence. *J. Biochem.* **112**, 314-320
11. Artavanis-Tsakonas, S., Matsuno, K., and Fortini, M.E. (1995) Notch signaling. *Science* **268**, 225-232
12. Fortini, M.E. and Artavanis-Tsakonas, S. (1994) The Suppressor of Hairless protein participates in Notch receptor signaling. *Cell* **79**, 273-282
13. Furukawa, T., Maruyama, S., Kawaichi, M., and Honjo, T. (1992) The *Drosophila* homolog of the immunoglobulin recombination signal-binding protein regulates peripheral nervous system development. *Cell* **69**, 1191-1197
14. Kato, H., Sakai, T., Tamura, K., Minoguchi, S., Shirayoshi, Y., Hamada, Y., Tsujimoto, Y., and Honjo, T. (1997) Involvement of RBP-J in biological functions of mouse Notch1 and its derivatives. *Development* **124**, 4133-4141
15. Luis de la Pompa, J., Wakeham, A., Correia, K.M., Samper, E., Brown, S., Aguilera, R.J., Nakano, T., Honjo, T., Mak, T.W., Rossant, J., and Conlon, R.A. (1997) Conservation of the Notch signalling pathway in mammalian neurogenesis. *Development* **124**, 1139-1148
16. Schweisguth, F. and Posakony, J.W. (1992) Suppressor of Hairless, the *Drosophila* homolog of the mouse recombination signal-binding protein gene, controls sensory organ cell fates. *Cell* **69**, 1199-1212
17. Grossman, S., Johannsen, E., Tong, X., Yalamanchili, R., and Kieff, E. (1994) The Epstein-Barr virus nuclear antigen 2 transactivator is directed to response elements by the Jκ recombination signal binding protein. *Proc. Natl. Acad. Sci. USA* **91**, 7568-7572
18. Henkel, T., Ling, P.D., Hayward, S.D., and Peterson, M.G. (1994) Mediation of Epstein-Barr virus EBNA2 transactivation by recombination signal-binding protein Jκ. *Science* **265**, 92-95
19. Waltzer, L., Logeat, F., Brou, C., Israel, A., Sergeant, A., and Manet, E. (1994) The human Jκ recombination signal sequence binding protein (RBP-Jκ) targets the Epstein-Barr virus EBNA2 protein to its DNA responsive elements. *EMBO J.* **13**, 5633-5638
20. Zimber-Strobl, U., Strobl, L.J., Meitinger, C., Hinrichs, R., Sakai, T., Furukawa, T., Honjo, T., and Bornkamm, G.W. (1994) Epstein-Barr virus nuclear antigen 2 exerts its transactivating function through interaction with recombination signal binding protein RBP-Jκ, the homologue of *Drosophila* Suppressor of Hairless. *EMBO J.* **13**, 4973-4982
21. Minoguchi, S., Taniguchi, Y., Kato, H., Okazaki, T., Strobl, L.J., Zimber-Strobl, U., Bornkamm, G.W., and Honjo, T. (1997) RBP-L, a transcription factor related to RBP-Jκ. *Mol. Cell. Biol.* **17**, 2679-2687
22. Tun, T., Hamaguchi, Y., Matsunami, N., Furukawa, T., Honjo, T., and Kawaichi, M. (1994) Recognition sequence of a highly conserved DNA binding protein RBP-Jκ. *Nucleic Acids Res.* **22**, 965-971
23. Hsieh, J.J., Henkel, T., Salmon, P., Robey, E., Peterson, M.G., and Hayward, S.D. (1996) Truncated mammalian Notch1 activates CBF1/RBP Jκ-repressed genes by a mechanism resembling that of Epstein-Barr virus EBNA2. *Mol. Cell. Biol.* **16**, 952-959
24. Kato, H., Sakai, T., Tamura, K., Minoguchi, S., Shirayoshi, Y., Hamada, Y., Tsujimoto, Y., and Honjo, T. (1996) Functional conservation of mouse Notch receptor family members. *FEBS Lett.* **395**, 221-224
25. Tamura, K., Taniguchi, Y., Minoguchi, S., Sakai, T., Tun, T., Furukawa, T., and Honjo, T. (1995) Physical interaction between a novel domain of the receptor Notch and the transcription factor RBP-Jκ/Su(H). *Curr. Biol.* **5**, 1416-1423
26. Sambrook, J., Fritsch, E.F., and Maniatis, T. (1989) *Molecular Cloning. A Laboratory Manual*, pp. 1339-1341, 2nd ed., Cold Spring Harbour Laboratory Press, Cold Spring Harbour, NY
27. Kimura, S., Niwa, H., Moriyama, M., Araki, K., Abe, K., Miike, T., and Yamamura, K. (1994) Involvement of germ line transmission by targeting β-galactosidase to nuclei in transgenic mice. *Dev. Growth Differ.* **36**, 521-527
28. Gomi, H., Yokoyama, T., Fujimoto, K., Ikeda, T., Katoh, A., Itoh, T., and Itohara, S. (1995) Mice devoid of the glial fibrillary acidic protein develop normally and are susceptible to scrapie prions. *Neuron* **14**, 29-41
29. Palmer, T.D., Takahashi, J., and Gage, F.H. (1997) The adult rat hippocampus contains primordial neural stem cells. *Mol. Cell Neurosci.* **8**, 389-404
30. Suzuki, S.C., Inoue, T., Kimura, Y., Tanaka, T., and Takeichi, M. (1997) Neuronal circuits are subdivided by differential expression of type-II class cadherins in postnatal mouse brains. *Mol. Cell. Neurosci.* **9**, 433-447
31. Kaneko, T., Itoh, K., Shigemoto, R., and Mizuno, N. (1989)

Glutaminase-like immunoreactivity in the lower brainstem and cerebellum of the adult rat. *Neuroscience* **32**, 79-98
32. Kaneko, T., Urade, Y., Watanabe, Y., and Mizuno, N. (1987) Production, characterization, and immunohistochemical application of monoclonal antibodies to glutaminase purified from rat brain. *J. Neurosci.* **7**, 302-309
33. Kaneko, T., Urade, Y., and Mizuno, N. (1988) Correlation between immunochemical characteristics and immunohistochemical applicability of nine lines of monoclonal antibodies against rat brain glutaminase. *J. Histochem. Cytochem.* **36**, 997-1004
34. Morris, R.G.M., Garrud, P., Rowlins, J.N.P., and O'Keefe, J. (1982) Place navigation impaired in rats with hippocampal lesions. *Nature* **297**, 681-683
35. Kawaichi, M., Oka, C., Shibayama, S., Koromilas, A.E., Matsunami, N., Hamaguchi, Y., and Honjo, T. (1992) Genomic organization of mouse Jκ recombination signal binding protein (RBP-Jκ) gene. *J. Biol. Chem.* **267**, 4016-4022
36. Kaneko, T., Nakaya, Y., and Mizuno, N. (1992) Paucity of glutaminase-immunoreactive nonpyramidal neurons in the rat cerebral cortex. *J. Comp. Neurol.* **322**, 181-190
37. Kaneko, T. and Mizuno, N. (1994) Glutamate-synthesizing enzymes in GABAergic neurons of the neocortex: a double immunofluorescence study in the rat. *Neuroscience* **61**, 839-849
38. Aster, J.C., Robertson, E.S., Hasserjian, R.P., Turner, J.R., Kieff, E., and Sklar, J. (1997) Oncogenic forms of NOTCH1 lacking either the primary binding site for RBP-Jκ or nuclear localization sequences retain the ability to associate with RBP-Jκ and activate transcription. *J. Biol. Chem.* **272**, 11336-11343
39. Tani, S., Taniwaki, M., Taniguchi, Y., Minoguchi, S., Kuroda, K., Han, H., Aoki, T., Miyatake, S., Hashimoto, N., and Honjo, T. (1998) Chromosomal mapping of two RBP-J-related genes: Kyo-T and RBP-L. *J. Hum. Gen.* **44**, 73-75